Materials Express

2158-5849/2020/10/892/011
doi:10.1166/mex.2020.1728
www.aspbs.com/mex

Article

Poly(ε-caprolactone)/graphene oxide composite systems: A comparative study on hydrolytic degradation at extreme pH values

Alberto J. Campillo-Fernández[1], Pablo González-Reed[1], Ana Vidaurre[1,2], and Isabel Castilla-Cortázar[1,*]

[1]*Centro de Biomateriales e Ingeniería Tisular, Universitat Politècnica de València, 46022 Valencia, Spain*
[2]*CIBER de Bioingeniería, Biomateriales y Nanomedicina (CIBER-BBN), Madrid, 28029, Spain*

ABSTRACT

Polycaprolactone/Graphene oxide (PCL/GO) composites are shown to be promising substrates for tissue engineering as their degradation behavior is a key aspect in this type of application. The present paper studies the effect of different GO contents (0.1, 0.2 and 0.5 wt%) of PCL/GO composites on accelerated hydrolytic degradation at extreme pH values. Degradation kinetics at pH 13 is strongly affected by GO content, and speed up at higher percentages. The composite with 0.5 wt% of GO was completely degraded in 72 hours, while degradation at pH 1 presents a different profile and seems to have an induction period that lasts more than 1500 hours. Morphological changes, molecular weight distribution, weight loss, degree of swelling and calorimetric properties were investigated as a function of degradation time. According to the results obtained, the addition of small percentages of GO significantly influences the degradation behavior of the composites acting as degradation modulators.

Keywords: Polycaprolactone, Graphene Oxide, Nanocomposite, Hydrolytic Degradation, Accelerated Degradation.

1. INTRODUCTION

Graphene oxide (GO) is a widely studied form of graphene that contains hydroxyl, carboxyl and epoxide functional groups on the surface of its sheets, which can improve its solubility, processability and interactions with organic polymers [1–4].

Polymer/GO nanocomposites have higher mechanical, thermal, gas barrier, chemical resistance, electrical and flame retardant properties than neat polymers. The improved electrical and mechanical properties of graphene-based nanocomposites have been reported to be better than those of clay or other carbon-based polymer nanocomposites [4–6]. Some studies have found that suspended hydrophobic graphene particles, which are poorly dispersible in aqueous media, are more toxic than hydrophilic graphene oxide (GO) or functionalized graphene [7]. GO-polymer's remarkable properties make it highly suitable for use in tissue engineering and regenerative medicine [8–11]. The functional GO groups can be thermally or chemically reduced to produce reduced GO (RGO), which has much higher conductivity than GO [10, 12].

GO has been proven to be a biocompatible nanomaterial, while the presence of metallic impurities within carbon nanotubes (CNTs) can cause toxicological effects [13]. Although GO could be considered as a biocompatible nanomaterial, further research is undergoing to understand the details of its probable toxicity and side effects in order to minimize its potential risks in clinical applications [14–15].

*Author to whom correspondence should be addressed.

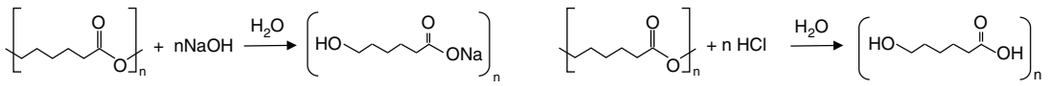

Fig. 1. Hydrolytic degradation of poly(ε-caprolactone) under alkaline (left) and acidic (right) conditions.

Poly(ε-caprolactone) (PCL) is a synthetic biodegradable polyester extensively used in biomedical applications [16–21]. Sayyar et al. [17] investigated two methods for the synthesis of polycaprolactone graphene composites, obtaining covalently linked materials with good solubility and processability, which makes them good candidates for use in tissue engineering. Hassanzadeh et al. [19] synthesized biobased 2D GO quantum dots and demonstrated their ability to promote mineralization, and also explored the potential of the prepared PCL nanocomposites as bone tissue scaffolds. Kumar et al. [21] prepared and characterized the cellular response to PCL/GO nanocomposites intended for orthopedic applications. Reinforcement of GO and RGO nanoparticles in PCL improves their mechanical and surface properties [18, 22] and influences surface water wettability [8, 21]. Diban et al. [23] produced PCL-GO membranes using phase inversion techniques, nontoxic reagents and mild temperature conditions for use in neural tissue engineering bioreactors.

Göpferich defines polymer degradation as the chemical reaction that brings about the cleavage of the polymer chains, producing oligomers and finally monomers [24]. According to the same author, erosion produces the loss of material as oligomers and monomers leave the polymer. PCL has been found to degrade in different ways, including chemical hydrolysis, microbial, enzymatic and thermal degradation, starting either on the surface (homogeneous) or in the interior (heterogeneous). The process depends on different parameters, e.g., chemical composition, chain orientation, molecular weight distribution, surface properties, hydrophilicity, presence of residual monomers and the environmental degradation conditions (temperature, relative humidity, pH) [25–28].

Nanofillers may affect the degradation rate of PCL and other polyesters, in either direction according to the effect of the filler used on crystallization and hydrophobicity of the polymer matrix [29–31]. A literature review reveals that there is great confusion, and even contradictory results, in the studies on the degradation of PCL nanocomposites [32]. Some authors [29, 33–36] have found an increased degradation rate with the addition of nanofillers, other than GO, on the degradation of aliphatic polyesters, while still others [37–41] have found that non-GO nanofillers slowed down or retarded the degradation of other aliphatic polyesters during either hydrolytic degradation or biodegradation. Unfortunately, no systematic reports have been published so far on the biodegradability of aliphatic polyester/GO samples [15].

Murray et al. studied the enzymatic degradation of graphene/PCL to study the effects of added graphene on the degradation rates of the corresponding nanocomposite scaffolds. A low concentration of RGO (<1 wt%) did not change the enzymatic degradation rate of PCL/RGO composites, but at higher concentrations, degradation slowed down [42]. Balkova et al. carried out a 21-day biodegradation experiment on the action of *Bacillus subtilis* on poly(ε-caprolactone) composite with GO [43]. According to Patel et al. [44], graphene-PCL nanocomposites and their 8-week-old degradation products were found to be highly cytocompatible and aided the adhesion and proliferation of C2C12 mouse myoblast cells. The degraded scaffolds were subjected to mechanical testing to evaluate the changes in the elastic modulus and the ultimate tensile strength of nanocomposites during *in vitro* degradation.

Degradation can be speeded up by using an acidic or alkaline medium to facilitate the study of morphological and chemical changes during the process. According to Lam et al. [45], this method would be better than other ones to mimic physiological conditions. In addition, degradation at different pH values is of interest in tissue engineering applications because of the wide range of pH found in the body. In the stomach it can be as low as 0.9–1.5 while in the duodenum it ranges between 7.5 and 8.5 [46].

Hydrolytic degradation in alkaline or acidic conditions breaks the polymeric chains through the ester bonds. Hydrolytic degradation under these conditions is shown in Figure 1.

Alkaline media have been used to study polymer hydrolysis [47–48], whose reactions can be catalyzed by both acids and alkalis [24, 48]. To our knowledge, no studies on the accelerated degradation of PCL/GO composites have yet been published.

The present study is the continuation of previous work [49] in which PCL/GO composites were produced by the solution mixing method. In order to advance in the comprehension of PCL/GO composite materials different properties were analyzed.

In this work the aim is to explore the effects of low GO percentages on the accelerated degradation of PCL/GO composites in terms of modulating the degradation. The effects of small percentages of GO were assessed on degradation at acidic, pH 1, and basic, pH 13, based on morphological changes, weight loss, degree of swelling, molecular weight distribution and calorimetric properties, in an attempt to understand the effects of incorporating GO into the degradability of the composites.

Article

2. EXPERIMENTAL DETAILS

2.1. Preparation of PCL/GO Composites

PCL pellets from Sigma-Aldrich ($M_w = 70{,}000$–$90{,}000$), dioxane solvent from Fisher and graphene oxide powder with a particle size of around 15 microns from Graphenea were used as received.

2.2. Degradation Solutions

Hydrochloric acid (HCl) and sodium hydroxide (NaOH) from Sharlab were used as received. Distilled water was used as a solvent to prepare 2.5 M HCl (pH 1) and 2.5 M NaOH (pH 13) degradation solutions.

2.3. PCL/GO Composites Preparation

After dissolving PCL in dioxane it was mixed with solutions containing three different proportions of GO dispersed in dioxane (0.1, 0.2, and 0.5% w/w GO/PCL) following the method used in our previous study [49]. The samples were labeled according to the percentage of GO as follows: PCL (neat PCL), PCL/GO-0.1 (0.1 wt.% of GO), PCL/GO-0.2 (0.2 wt.% of GO), and PCL/GO-0.5 (0.5 wt.% of GO). Mean sheet thickness was 2 mm.

2.4. Incubation into Degradation Solutions

The degradation procedure of cylindrical samples (diameter, 5 mm; thickness, 2 mm) was the same as in our previous study [50]. Briefly, samples (≈55 mg) were placed in test-tubes containing 10 mL of degradation solution at either pH 1 or pH 13. As the PCL/GO-0.5 samples could not be punched to produce the discs due to the brittle nature of the material, instead they were carefully cut into approximately cylindrical shapes. The degradation process took place in an oven maintained at 37 °C, and reached a maximum incubation period of 1700 hours for both pH values. At different time intervals, three sample replicates were taken out of the degradation solution, washed thoroughly with distilled water, gently wiped with blotting paper to eliminate surface water, weighed and subsequently vacuum dried to constant weight before analysis.

2.5. Morphology: Scanning Electron Microscopy (SEM)

The surface and transversal morphology of dried samples was studied in SEM images of non-degraded and degraded samples at all degradation times, by means of a JEOL JSM-5410 (Tokyo, Japan) scanning electron microscope. The samples, previously gold sputter-coated, were monitored at 10 kV of acceleration voltage and 15 mm working distance.

2.6. Degree of Swelling and Weight Loss

After degradation, the water absorbed by the materials and weight loss were determined. The samples were rinsed with distilled water and wiped with blotting paper. Wet weight was measured to assess the changes in the hydrophilicity of the samples. The samples were dried in a vacuum oven, at room temperature, until constant weight, and the degree of swelling was obtained by comparing the wet weight (w_w) with dry weight (w_d) at a certain time, according to Eq. (1):

$$\text{degree of swelling } (\%) = \frac{w_w - w_d}{w_d} \times 100 \qquad (1)$$

The percentage weight loss respect to the initial weight (w_0) was determined at a specific degradation time, according to Eq. (2):

$$\text{weight loss } (\%) = \frac{w_0 - w_d}{w_0} \times 100 \qquad (2)$$

A Mettler Toledo semi microbalance with a readability of 0.01 mg was used to weigh the samples.

2.7. Molecular Weight Analysis by Gel Permeation Chromatography (GPC)

The evolution of the weight average molecular weight of the samples was determined by GPC on a Waters Breeze GPC system with a 1525 Binary HPLC pump (Waters Corporation, Milford, MA, USA) equipped with a 2414 refractive index detector and Waters Styragel HR THF columns. As eluent, a constant flow rate of 1 mL/min of tetrahydrofuran (THF) at 30 °C was used. The calibration curve was prepared according to Shodex monodisperse polystyrene standards (Showa Denko K.K. Kawasaki, Japan). PCL molecular weights were taken from the Mark-Houwink-Sakurada parameters provided by Huang et al. [51] ($k = 2.9 \cdot 10^{-4}$ [dL/g], $\alpha = 0.7$).

2.8. Differential Scanning Calorimetry (DSC)

The samples' thermal properties were studied on a Mettler Toledo differential scanning calorimeter (DSC, Perkin Elmer, Überlingen, Germany) calibrated with indium. The measurements were taken at a scan rate of 10 °C/min between −10 °C and 100 °C. Crystallinity was calculated assuming proportionality to the experimental heat of fusion, considering 139.5 J/g for the 100% crystalline neat PCL [52].

3. RESULTS AND DISCUSSION

3.1. Visual Examination and SEM

The neat PCL was white in color while the composite samples were uniformly brown, which became darker as GO concentration increased. Prior to degradation, sample surfaces were practically smooth and even (see Fig. 2).

The microstructure of the surfaces of the prepared samples were monitored by SEM. The morphological degradation of the surface of the samples was evident and became increasingly eroded at higher GO content (see, by way of example, Fig. 3). Small cavities can be seen in the neat PCL (first column in Fig. 3) after 143 h when weight loss

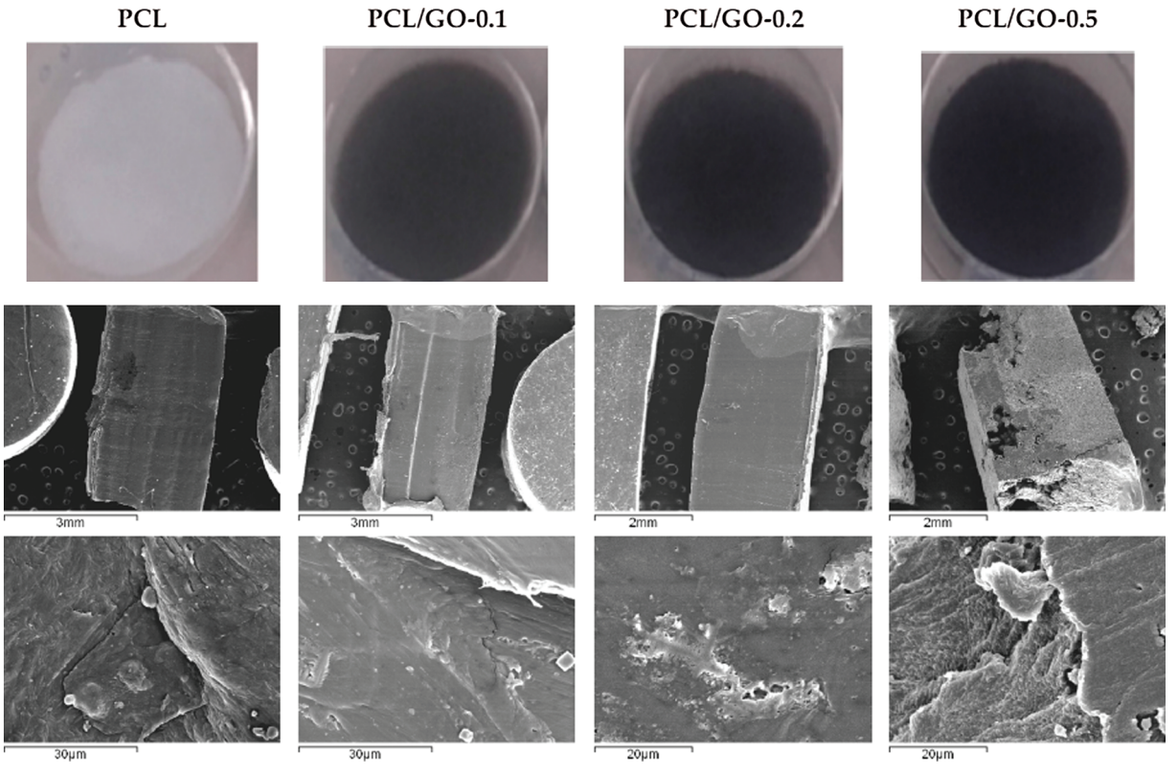

Fig. 2. Sample photographs (above) and transversal SEM images according to GO content. Extracted from Ref. [49], Castilla-Cortázar, I., et al., **2019**. Morphology, crystallinity, and molecular weight of poly(ε-caprolactone)/graphene oxide hybrids. *Polymers, 11*, p.1099.

was 6.17%. The composite PCL/GO-0.1 (second column in Fig. 3) presented larger hollow regions, pores and insets containing enlargements created by the reaction of OH groups with the polymeric chains. The trend is confirmed by the degradation in the composite PCL/GO-0.2, as can be seen in the third column in Figure 3. And also, because after 143 h no mass remain of the composite PCL/GO-0.5. It should be noted that GO sheets were left behind in the solution in which the PCL/GO-0.5 composite had been degraded and its color changed to grayish-black due to the GO sheets.

Visual and SEM inspection of the samples incubated at pH 1 revealed a uniform surface and cross-sections, leaving the overall sample structure and architecture intact. The overall gross morphology of the samples was not visibly different to their initial state. As can be seen in Figure 4, after 889 hours of degradation the upper surface appeared to have uniform defects. There were no evident signs of degradation.

3.2. Weight Loss

The weight loss profiles of neat PCL and PCL/GO composites measured at 37 °C as a function of time and pH are shown in Figure 5. It can be seen that, at pH 13, before 625 hours mass loss increases with the percentage of GO, probably because the GO acts as a reactive site due to its functional groups, through which the OH groups of the NaOH solution can react with the matrix. At longer degradation times, the percentage weight loss is similar for the PCL/GO-0.1, and PCL/GO-0.2 composites and neat PCL, as can be seen in Figure 5(a). It can be observed that there were two weight loss rates, which were initially fast, and then slowed down after 625 hours, when approximately 80% of the initial mass had been lost. In the composite PCL/GO-0.5, the samples degraded rapidly and no mass remained at 72 hours.

However, the samples degraded at pH 1 hardly changed throughout the degradation period, as can be seen in Figure 5(b). The weight loss of neat PCL is less than 2% for the whole degradation period.

Samples containing GO reached the maximum weight loss of around 4% after 1700 hours for PCL/GO-0.5. On the other hand, PCL/GO-0.1 and PCL/GO-0.2 samples followed the same trend in which the weight loss did not significantly change and was less than 2% over the whole degradation period, which means that the overall rate of weight loss was extremely slow. Statistical differences between weight losses of the different samples were determined by a nonparametric Kruskal–Wallis test for each degradation time. The statistical analysis found no significant differences ($p > 0.05$) between the degradation rate of neat PCL and PCL/GO-0.1 and the rest of the samples.

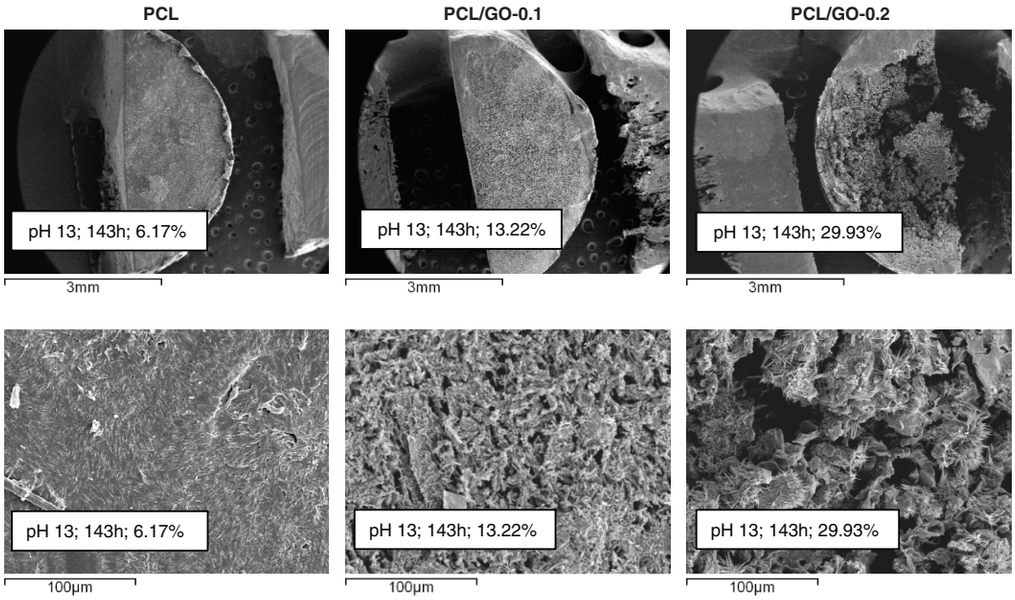

Fig. 3. SEM microphotographs of the upper surface of the samples after being submitted to the same degradation time ($t = 143$ h) at pH 13. From left to right: PCL, PCL/GO-0.1, PCL/GO-0.2. (Top row bar = 3 mm, bottom row bar = 100 μm).

PCL degradation is generally accepted to be due to hydrolytic cleavage of the ester bonds. When the ester bonds in the polymer chains react with water molecules, the length of the degraded chains is reduced. This ends in the short fragments of chains containing carboxylic end groups that make the polymer soluble in water [53].

The mechanism is based on the hydronium (H^+) and hydroxyl (OH^-) balance in the medium. At pH 7 this balance is neutral and the hydrolysis is prolonged over time. However, reports suggest that hydrolysis accelerates at pH 1 (higher H^+ content) and at pH 13 (higher OH^- content) [50].

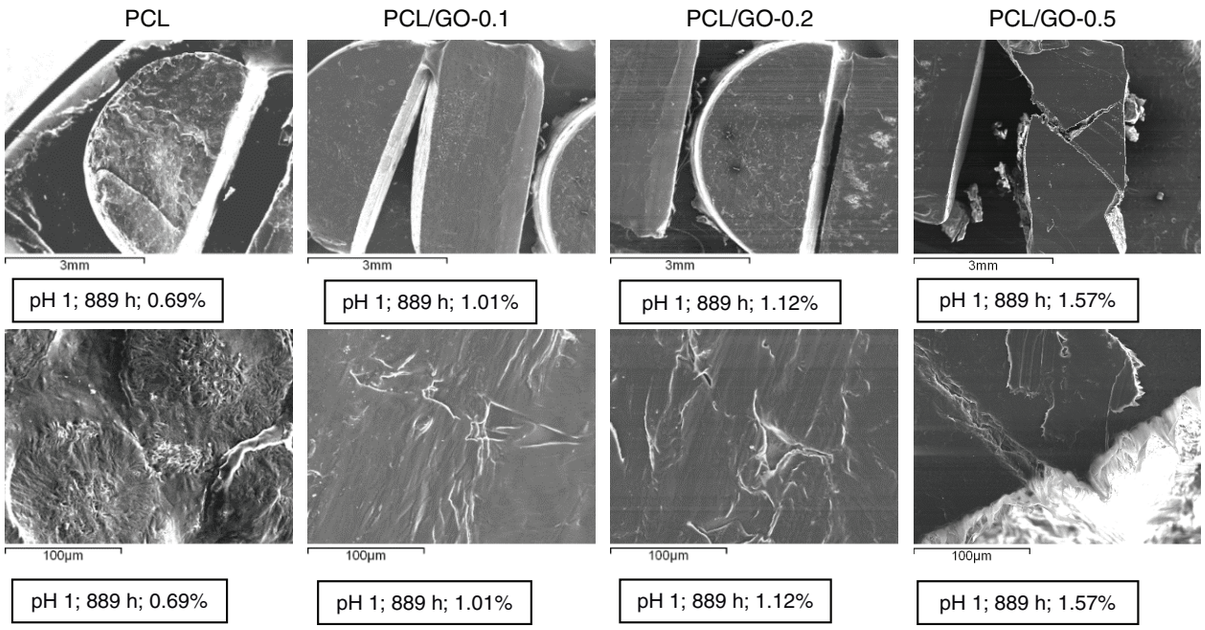

Fig. 4. SEM microphotographs of the upper surface of the samples after being submitted to the same degradation time ($t = 889$ h) at pH 1. From left to right: PCL, PCL/GO-0.1, PCL/GO-0.2. (Top row bar = 3 mm, bottom row bar = 100 μm).

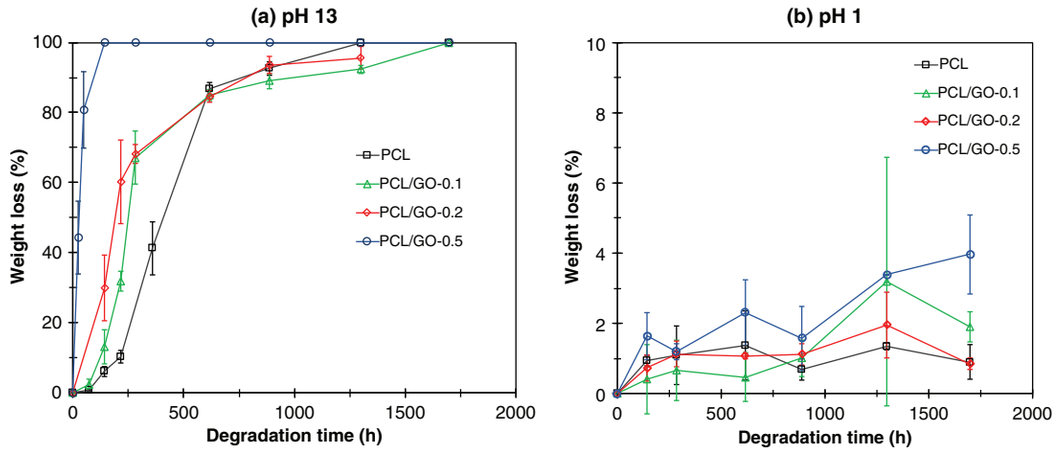

Fig. 5. Weight loss profile as a function of degradation time in: (a) Alkaline medium pH 13, (b) acid medium pH 1. Error bars represent standard deviation. Black: PCL; green: PCL/GO-0.1; red: PCL/GO-0.2; blue: PCL/GO-0.5.

According to our results for pH 1 (see Fig. 5(b)) with samples of neat PCL ($M_w = 70,000$–$90,000$) there seems to be an induction period that lasts for the total degradation period measured here, more than 1500 h. In the Sailema-Palate paper [50], the weight loss of neat PCL sheets ($M_w = 43,000$–$50,000$), degraded at pH 1, presented a clear induction period of around 300 h, after which the hydrolysis reaction progressed and the weight loss increased continuously to around 97% after 2300 h. According to the literature, degradation is significantly affected by initial molecular weight [54] and this effect depends on the type of hydrolysis mechanism [55]. It was found that the weight loss decreased as initial molecular weight increased, if weight loss was attributed to end scission. Here, with samples of PCL with a larger molecular weight, the induction period is expected to be longer.

However, as stated above, the addition of nanofillers such as GO can alter the polymer degradation behavior [29], which is the subject of the present paper. Indeed, when the samples are put in a solution at pH 13 (high availability of OH^-) degradation of the samples is faster at higher percentages of GO, as can be seen in Figure 5(a). These results can be explained by GO's flat structure with oxygenated functional groups (OHs, among others) on its surface. As has been shown by Dimiev et al. [56], when GO is placed in an alkaline solution (NaOH) there is a break in the GO's C–C bonds and H^+ ions are released into the medium. The latter are available to react with the PCL chains and break the ester bond, so the process can be seen as the superposition of an alkaline degradation and an acidic degradation. The process speeds up at higher GO contents. The presence of GO sheets in the polymer matrix seems to accelerate composite degradation by either acting as an anchor point through which the –OH groups can react with the polymeric matrix, or by altering the structure of the matrix, making it more porous, separating the polymer chains and creating "tunnels" through which the –OH groups can access the matrix and freely react with the polymer chains. This may explain the fact that the composite PCL/GO-0.5 was completely degraded before being taken out of the degradation medium after 72 hours.

The situation is completely different at pH 1, since GO in aqueous acidic solution (HCl) is reduced by consuming H^+ and releasing Cl_2 (g), which reduces the availability of hydroniums to break the PCL bonds. As seen in Figure 5(b), the induction period is so long that no loss of mass is apparent in the time interval studied. GO's hydrophilic nature [3, 57] could possibly facilitate water penetration (PCL is hydrophobic) and thus make a slight contribution to degradation.

3.3. Degree of Swelling

The pH of the degradation solution influenced the degrees of swelling of the degraded samples. As more water penetrates the samples, swelling increases the hydrolysis rate. As can be seen in Figure 6(a), for samples of neat PCL degraded at pH 13 the amount of water in the sample rose to a maximum value of around 20% in a period of 625 hours.

The composite samples PCL/GO-0.1 showed an initial increase and reached a maximum degree of swelling of 14.5% in a period of 284 hours. The composite samples PCL/GO-0.2 showed a similar trend. The degree of swelling in the PCL/GO-0.5 composites at pH 13 could not be studied at degradation times longer than 72 hours because the samples had completely degraded after that time (Fig. 6(a)). The statistical analysis shows significant differences between the degree of swelling of PCL/GO-0.1 and PCL/GO-0.2, but no significant differences with the rest of the samples.

Figure 6(b) shows the swelling degree as a function of degradation time in acid medium pH 1. The samples of

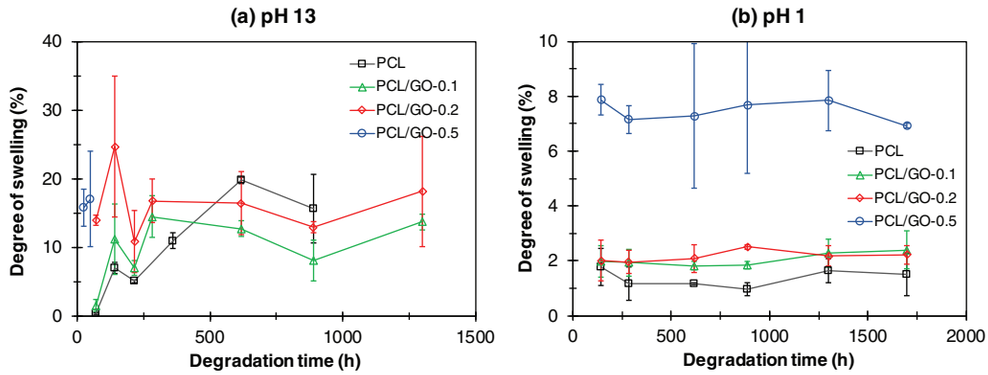

Fig. 6. Degree of swelling as a function of degradation time in: (a) Alkaline medium pH 13, (b) acid medium pH 1. Error bars represent standard deviation. Black: PCL; green: PCL/GO-0.1; red: PCL/GO-0.2; blue: PCL/GO-0.5.

neat PCL showed a small initial increase in the swelling degree of up to approximately 1% at 143 hours, and stayed constant for the rest of the experiment, which is consistent with the weight loss profile. The behavior of PCL/GO-0.1, and PCL/GO-0.2 composites in acid medium was practically identical. In the PCL/GO-0.5 samples immersed in pH 1 solution the degree of swelling initially rose to approximately 8% and stayed between 7 and 8% throughout the rest of the experiment. This can be explained by the more hydrophilic behavior of GO and the fact that it produces a more porous structure that allows the water to enter the matrix much more easily than in the composites with lower GO content. The comparison of the degree of swelling in the degradation at pH 1 and pH 13 shows the effect of porosity produced by degradation of the composites at pH 13. The degree of swelling of the samples degraded at pH 13 is more than twice the highest value at pH 1 for PCL/GO-0.5 and up to 10–15 times more for the rest of the samples.

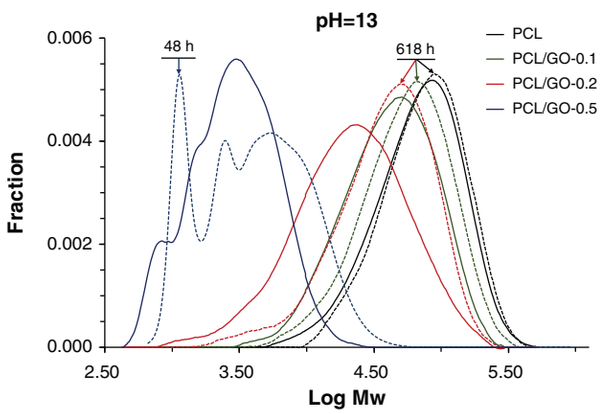

Fig. 7. Molecular weight distribution as a function of GO content and degradation time for pH 13. Solid lines represent samples' M_w prior to degradation while dotted lines represent samples' M_w after degradation (degradation time indicated). Black: PCL; green: PCL/GO-0.1; red: PCL/GO-0.2; blue: PCL/GO-0.5. Degradation time equals 618 hours for all samples, except for PCL/GO-0.5, which is 48 hours.

3.4. Molecular Weight Analysis

Figure 7 shows the molecular weight distribution of the degraded samples in pH 13 solution at 618 hours for PCL, PCL/GO-0.1, and PCL/GO-0.2, and after 48 hours for the PCL/GO-0.5 sample. It can be seen that while the PCL molecular weight distribution did not change, the molecular weight distribution of the composite samples moved towards higher molecular weights. As the GO content increases, the profile presents the superposition of different molecular weight distributions, with an increase in the contribution of the smaller weight distribution. This is most remarkable in the composite with the highest GO content, in which the superposition of three molecular weight distributions can be seen.

The results of the average molecular weight for two different degradation times, shown in Table I, confirm the results shown in Figure 7. Before degradation, as the GO content increases, the apparent molecular weight decreases, ranging from 97095 for pure PCL to 4436 for PCL/GO-0.5. This surprising effect was explained in our previous work [49], and was attributed to the PCL-GO interaction. The displacement towards a higher molecular weight with degradation can be explained by the effect of

Table I. Degradation time, t_d, molecular weight, M_w, for composites with different GO content at pH 13.

Sample	t_d (hours)	M_w
PCL	0	97095
	143	91334
	618	96567
PCL/GO-0.1	0	61472
	143	65290
	618	73436
PCL/GO-0.2	0	37878
	143	51134
	618	54079
PCL/GO-0.5	0	4436
	24	6376
	48	5748

Article

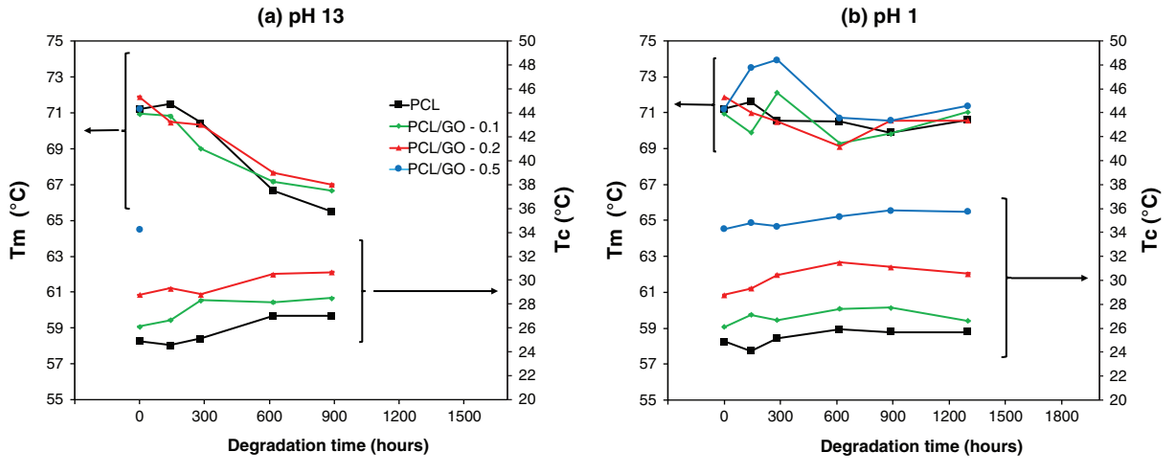

Fig. 8. Crystallization temperature, T_c, and melting temperature, T_m, of the first heating scan of the composites at different degradation times at pH 13 (a), and pH 1 (b).

GO on the measurement of the apparent molecular weight by GPC. Thus, as degradation proceeds, part of the GO content is released from the sample into the degradation medium (as shown by its grayish-black color). The results of the molecular weight measurements indicate that the percentage of GO could decrease with degradation.

The molecular weight distribution of the samples degraded in immersion at pH 1 did not show any differences with the corresponding non-degraded samples (data not shown). This is consistent with the fact that degradation had not started after 1700 hours in the acidic degradation medium.

3.5. Differential Scanning Calorimetry

Figure 8 shows the melting temperatures of the first heating scan of the PCL/GO composites, T_m, and the crystallization temperature, T_c, as a function of time and pH, Figure 8(a) at pH 13 and Figure 8(b) at pH 1. As can be seen at pH 1, the composites do not present variations of the melting peak temperature with degradation time or GO content, Figure 8(b). However, GO has a clear influence on T_c, as the greater the amount of GO, the higher the T_c, indicating the nucleating effect of the GO sheets, as reported in previous studies [21, 49, 58–59]. GO has been found to increase the number of crystallization nucleation sites and modify the number and size of spherulite crystalline regions in PCL [17, 49]. In short, at pH 1 only GO content has an influence on the composites, since degradation has only just begun in these conditions. However, at pH 13, see Figure 8(a), the melting temperatures are clearly seen to fall as degradation progresses, indicating smaller crystals. As at pH 1, crystallization temperature is evidently influenced by GO content, see Figure 8(b). The higher the GO content the higher the crystallization temperature [49], which remains fairly constant throughout the degradation process.

It should be noted that when the samples were immersed in the degradation medium, crystallinity underwent certain fluctuations. As can be seen in Figures 9(a) and (b), the crystallinity of the composites degraded at pH 13 and pH 1 remained fairly constant.

The fact of adding low GO percentages to the PCL involves some differences in accelerated degradation at extreme pHs. First of all, degradation of PCL/GO composites at pH 13 is much faster and increases with GO content, Figure 5(a). At pH 1, Figure 5(b), there seems to be an induction period that lasts more than 1500 hours, i.e., the entire time interval studied, in which the loss of mass is less than 2%, except for the sample PCL/GO-0.5, while there are no appreciable changes in crystallinity, melting temperature and crystallization, as can be seen in Figures 8(b) and 9(b). The fact that after 1500 h the PCL/GO samples degraded at pH 13 have completely degraded while those degraded at pH 1, after 1500 h, have not yet begun to degrade may be of great interest in tissue engineering as well as in controlled drug delivery.

The results of Sailema et al. [50] on neat PCL at pH 1, with higher weight loss and water absorption during degradation, including the findings on molecular weight distribution and changes in morphology, appeared to indicate a bulk erosion mechanism. After the induction phase, the molecules became water-soluble and the polymer lost 97% of its weight in approximately 2200 hours. However, at pH 13, the results of the degradation in molecular weight, weight loss, water uptake, DSC and morphology suggested a surface degradation mechanism [50].

In the present study, GO clearly plays the role of nucleating agent, with higher crystallization temperatures at higher GO contents. At pH 1, since degradation has not started, no changes can be seen in any calorimetric and other studied properties, while at pH 13 the degradation affects both the amorphous and crystalline phases. As degradation time increases, in addition to the amorphous

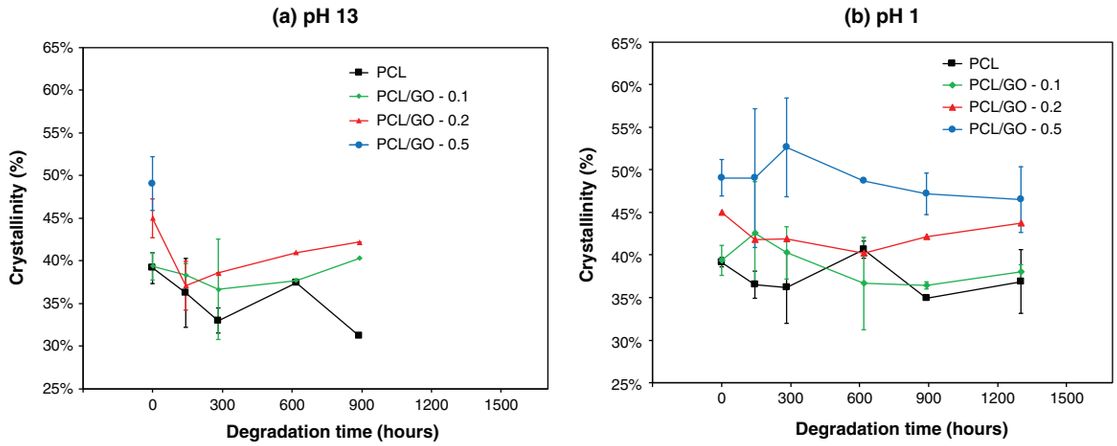

Fig. 9. Crystallinity of the composites on cooling as a function of degradation time at (a) pH 13, (b) pH 1.

phase degradation, the crystals become smaller through erosion, as corroborated by the reduced melting temperature in the first heating scan, Figure 8(a). From our results, Figures 3, 5(a), 6(a) and 9(a), it can be deduced that, at pH 13, the degradation proceeded via the mechanism of surface degradation.

In this study of accelerated degradation, the role of GO as a degradation modulator should be noted. Future research work will be carried out to determine evolution of degradation at pH 1.

4. CONCLUSIONS

This paper describes a study of the hydrolytic degradability of PCL sheets incorporating GO at different filler contents (0, 0.1, 0.2 and 0.5 wt%) in both an accelerated setting under alkaline conditions (pH 13) and accelerated degradation under acidic conditions (pH 1). In an accelerated setting, researchers may expect to obtain similar results by altering the rate of reaction whilst maintaining the principal reaction mechanisms. However, any data obtained in this way should always be verified by long-term data. The behavior of the composites in accelerated degradation varies according to whether it is acidic or alkaline. The results show that accelerated degradation in an alkaline medium, pH 13, increases with GO percentage. However, when degradation is under acidic conditions, pH 1, there is an induction period that lasts for the entire study period, during which no relevant change occurs. The molecular weight distribution of the composite samples degraded at pH 13 moved towards higher molecular weights as degradation proceeded. Taking into account the strong correlation between composition and molecular weight measured by GPC, this would indicate that the GO percentage is reduced with degradation time. The study of the calorimetric properties shows that at pH 13 crystallinity does not vary significantly throughout the degradation period, but melting temperature decreases as degradation progresses, indicating smaller crystal sizes and the degradation of both the amorphous and crystalline phases. Future work will be required on degradation at pH 1, including longer periods of time to assess the evolution of degradation after the induction period and how it is affected by GO.

Acknowledgments: Isabel Castilla-Cortázar and Alberto J. Campillo-Fernández are grateful for the support of the Spanish Ministry of Science, Innovation and Universities, through RTI2018-095872-B-C22/ERDF. Ana Vidaurre would like to express her gratitude for the support of the Spanish Ministry of Science and Education, through the MAT2016-76039-C4-1-R Project, and also the support from CIBER-BBN, an initiative funded by the Sixth National R&D&i Plan 2008–2011, Iniciativa Ingenio 2010, Consolider Program, CIBER Actions financed by the Instituto de Salud Carlos III with assistance from the European Regional Development Fund.

References and Notes

1. Hummers, W.S. and Offeman, R.E., **1958**. Preparation of graphitic oxide. *Journal of the American Chemical Society, 80*(6), p.1339.
2. Stankovich, S., Piner, R.D., Nguyen, S.B.T. and Ruoff, R.S., **2006**. Synthesis and exfoliation of isocyanate-treated graphene oxide nanoplatelets. *Carbon, 44*(15), pp.3342–3347.
3. Dreyer, D.R., Park, S., Bielawski, C.W. and Ruoff, R.S., **2010**. Graphite oxide. *Chemical Society Reviews, 39*(1), pp.228–240.
4. Kuilla, T., Bhadra, S., Yao, D., Kim, N.H., Bose, S. and Lee, J.H., **2010**. Recent advances in graphene based polymer composites. *Progress in Polymer Science, 35*(11), pp.1350–1375.
5. Stankovich, S., Dikin, D.A., Dommett, G.H.B., Kohlhaas, K.M., Zimney, E.J., Stach, E.A., Piner, R.D., Nguyen, S.T. and Ruoff, R.S., **2006**. Graphene-based composite materials. *Nature, 442*(7100), pp.282–286.
6. Wang, X., Liu, X., Yuan, H., Liu, H., Liu, C., Li, T., Yan, C., Yan, X., Shen, C. and Guo, Z., **2018**. Non covalently functionalized graphene strengthened poly(vinyl alcohol). *Materials and Design, 139*, pp.372–379.
7. Feng, L. and Liu, Z., **2011**. Graphene in biomedicine: Opportunities and challenges. *Nanomedicine, 6*(2), pp.317–324.

Article

8. Shin, S.R., Li, Y.C., Jang, H.L., Khoshakhlagh, P., Akbari, M., Nasajpour, A., Zhang, Y.S., Tamayol, A. and Khademhosseini, A., **2016**. Graphene-based materials for tissue engineering. *Advanced Drug Delivery Reviews, 105*, pp.255–274.
9. Kumar, S., Raj, S., Sarkar, K. and Chatterjee, K., **2016**. Engineering a multi-biofunctional composite using poly(ethyleneimine) decorated graphene oxide for bone tissue regeneration. *Nanoscale, 8*, pp.6820–6836.
10. Kumar, S., Raj, S., Kolanthai, E., Sood, A.K.K., Sampath, S. and Chatterjee, K., **2015**. Chemical functionalization of graphene to augment stem cell osteogenesis and inhibit biofilm formation on polymer composites for orthopedic applications. *ACS Applied Materials & Interfaces, 7*(5), pp.3237–3252.
11. Kumar, S. and Chatterjee, K., **2016**. Comprehensive review on the use of graphene-based substrates for regenerative medicine and biomedical devices. *ACS Applied Materials & Interfaces, 8*, pp.26431–26457.
12. Murray, E., Sayyar, S., Thompson, B.C., Gorkin III, R., Officer, D.L. and Wallace, G.G., **2015**. A bio-friendly, green route to processable, biocompatible graphene/polymer composites. *RSC Advances, 5*(56), pp.45284–45290.
13. Liu, W., Chai, S., Rahman, A. and Hashim, U., **2014**. Synthesis and characterization of graphene and carbon nanotubes: A review on the past and recent developments. *Journal of Industrial and Engineering Chemistry, 20*(4), pp.1171–1185.
14. Wang, K., Ruan, J., Song, H., Zhang, J., Wo, Y., Guo, S. and Cui, D., **2011**. Biocompatibility of graphene oxide. *Nanoscale Research Letters, 6*(1), pp.1–8.
15. Akhavan, O., **2016**. Graphene scaffolds in progressive nanotechnology/stem cell-based tissue engineering of nervous systems. *Journal of Materials Chemistry B, 4*, pp.3169–3190.
16. Woodruff, M.A. and Hutmacher, D.W., **2010**. The return of a forgotten polymer—Polycaprolactone in the 21st century. *Progress in Polymer Science, 35*, pp.1217–1256.
17. Sayyar, S., Murray, E., Thompson, B.C., Gambhir, S., Officer, D.L. and Wallace, G.G., **2013**. Covalently linked biocompatible graphene/polycaprolactone composites for tissue engineering. *Carbon, 52*, pp.296–304.
18. Wan, C. and Chen, B., **2011**. Poly(ϵ-caprolactone)/graphene oxide biocomposites: Mechanical properties and bioactivity. *Biomedical Materials, 6*(5), pp.055010–055017.
19. Hassanzadeh, S., Adolfsson, K.H., Wu, D. and Hakkarainen, M., **2016**. Supramolecular assembly of biobased graphene oxide quantum dots controls the morphology of and induces mineralization on poly(ε-caprolactone) films. *Biomacromolecules, 17*(1), pp.256–261.
20. Bianco, A., **2013**. Graphene: Safe or toxic? the two faces of the medal. *Angewandte Chemie-International Edition, 52*(19), pp.4986–4997.
21. Kumar, S., Azam, D., Raj, S., Kolanthai, E., Vasu, K.S., Sood, A.K. and Chatterjee, K., **2016**. 3D scaffold alters cellular response to graphene in a polymer composite for orthopedic applications. *Journal of Biomedical Materials Research-Part B Applied Biomaterials, 104*(4), pp.732–749.
22. Kai, W., Hirota, Y., Hua, L. and Inoue, Y., **2008**. Thermal and mechanical properties of a poly(e-caprolactone)/graphite oxide composite. *Journal of Applied Polymer Science, 107*, pp.1395–1400.
23. Diban, N., Sánchez-González, S., Lázaro-Díez, M., Ramos-Vivas, J. and Urtiaga, A., **2017**. Facile fabrication of poly(ϵ-caprolactone)/graphene oxide membranes for bioreactors in tissue engineering. *Journal of Membrane Science, 540*, pp.219–228.
24. Göpferich, A., **1996**. Mechanisms of polymer degradation and erosion. *Biomaterials, 17*(2), pp.103–114.
25. Hakkarainen, M., **2002**. Aliphatic polyesters: Abiotic and biotic degradation and degradation products. in *Degradable Aliphatic Polyesters*. New York, Berlin, Heidelberg, Springer-Verlag, Vol. 157, pp.113–138.
26. Fukushima, K., Abbate, C., Tabuani, D., Gennari, M., Rizzarelli, P. and Camino, G., **2010**. Biodegradation trend of poly(ϵ-caprolactone) and nanocomposites. *Materials Science and Engineering C, 30*(4), pp.566–574.
27. Bosworth, L.A. and Downes, S., **2010**. Physicochemical characterisation of degrading polycaprolactone scaffolds. *Polymer Degradation and Stability, 95*(12), pp.2269–2276.
28. Burkersroda, F.V., Schedl, L. and Göpferich, A., **2002**. Why degradable polymers undergo surface erosion or bulk erosion. *Biomaterials, 23*(21), pp.4221–4231.
29. Bikiaris, D.N., **2013**. Nanocomposites of aliphatic polyesters: An overview of the effect of different nano fi llers on enzymatic hydrolysis and biodegradation of polyesters. *Polymer Degradation and Stability, 98*(9), pp.1908–1928.
30. Peng, H., Han, Y., Liu, T., Tjiu, P. and He, C., **2010**. Morphology and thermal degradation behavior of highly exfoliated CoAl-layered double hydroxide/polycaprolactone nanocomposites prepared by simple solution intercalation. *Thermochimica Acta, 502*, pp.1–7.
31. Kumar, S. and Maiti, P., **2016**. Controlled biodegradation of polymers using nanoparticles and its application. *RSC Advances, 6*(72), pp.67449–67480.
32. Bikiaris, D.N., Nianias, N.P., Karagiannidou, E.G. and Docoslis, A., **2012**. Effect of different nanoparticles on the properties and enzymatic hydrolysis mechanism of aliphatic polyesters. *Polymer Degradation and Stability, 97*(10), pp.2077–2089.
33. Zhou, Q. and Xanthos, M., **2008**. Nanoclay and crystallinity effects on the hydrolytic degradation of polylactides. *Polymer Degradation and Stability, 93*, pp.1450–1459.
34. Grizzi, I., Garreau, H., Li, S. and Vert, M., **1995**. Hydrolytic degradation of devices based on poly(DL-lactic acid) size dependence. *Biomaterials, 16*(4), pp.305–311.
35. Singh, N.K., Purkayastha, B.D., Roy, J.K., Banik, R.M., Yashpal, M., Singh, G., Malik, S. and Maiti, P., **2010**. Nanoparticle-induced controlled biodegradation and its mechanism in poly(ϵ-caprolactone). *ACS Applied Materials and Interfaces, 2*(1), pp.69–81.
36. Chouzouri, G. and Xanthos, M., **2007**. In vitro bioactivity and degradation of polycaprolactone composites containing silicate fillers. *Acta Biomaterialia, 3*, pp.745–756.
37. Someya, Y., Kondo, N. and Shibata, M., **2007**. Biodegradation of poly(butylene adipate-co-butylene terephthalate)/layered-silicate nanocomposites. *Journal of Applied Polymer Science, 106*, pp.730–736.
38. Lee, S.R., Park, H.M., Lim, H., Kang, T., Li, X., Cho, W.J. and Ha, C.S., **2002**. Microstructure, tensile properties, and biodegradability of aliphatic polyester clay nanocomposites. *Polymer, 43*, pp.2495–2500.
39. Wu, T.M. and Wu, C.Y., **2006**. Biodegradable poly(lactic acid)/chitosan-modified montmorillonite nanocomposites: Preparation and characterization. *Polymer Degradation and Stability, 91*(9), pp.2198–2204.
40. Fukushima, K., Tabuani, D., Abbate, C., Arena, M. and Rizzarelli, P., **2011**. Preparation, characterization and biodegradation of biopolymer nanocomposites based on fumed silica. *European Polymer Journal, 47*, pp.139–152.
41. Nerantzaki, M., Papageorgiou, G.Z. and Bikiaris, D.N., **2014**. Effect of nanofiller's type on the thermal properties and enzymatic degradation of poly(ϵ-caprolactone). *Polymer Degradation and Stability, 108*, pp.257–268.
42. Murray, E., Thompson, B.C., Sayyar, S. and Wallace, G.G., **2015**. Enzymatic degradation of graphene/polycaprolactone materials for tissue engineering. *Polymer Degradation and Stability, 111*, pp.71–77.
43. Balkova, R., Hermanova, S., Voberkova, S., Damborsky, P., Richtera, L., Omelkova, J. and Jancar, J., **2014**. Structure and morphology of microbial degraded poly(e-caprolactone)/graphite oxide composite. *Journal of Polymers and the Environment, 22*, pp.190–199.

44. Patel, A., Xue, Y., Mukundan, S., Rohan, L.C., Sant, V., Stolz, D.B. and Sant, S., **2016**. Cell-instructive graphene-containing nanocomposites induce multinucleated myotube formation. *Annals of Biomedical Engineering, 44*(6), pp.2036–2048.
45. Lam, C.X., Savalani, M.M., Teoh, S.H. and Hutmacher, D.W., **2008**. Dynamics of in vitro polymer degradation of polycaprolactone-based scaffolds: Accelerated versus simulated physiological conditions. *Biomedical Materials, 3*(3), Article ID: 34108.
46. Chu, C.C., **1982**. A comparison of the effect of pH on the biodegradation of two synthetic absorbable sutures. *Annals of Surgery, 195*(1), pp.55–59.
47. Pitt, C.G., Chasalow, F.I., Hibionada, Y.M., Klimas, D.M., Park, T. and Carolina, N., **1981**. Aliphatic polyesters. I. The degradation of poly(ε-caprolactone) in vivo. *Journal of Applied Polymer Science, 26*(11), pp.3779–3787.
48. Li, S.M., Chen, X.H., Gross, R.A. and Mccarthy, S.P., **2000**. Hydrolytic degradation of PCL/PEO copolymers in alkaline media. *Journal of Materials Science: Materials in Medicine, 11*, pp.227–233.
49. Castilla-Cortázar, I., Vidaurre, A., Mari, B. and Campillo-Fernández, A.J., **2019**. Morphology, crystallinity, and molecular weight of poly(ε-caprolactone)/graphene oxide hybrids. *Polymers, 11*, Article ID: 1099.
50. Sailema-Palate, G.P., Vidaurre, A., Campillo, A.J. and Castilla-Cortázar, I., **2016**. A comparative study on poly(ε-caprolactone) film degradation at extreme pH values. *Polymer Degradation and Stability, 130*, pp.118–125.
51. Huang, Y., Xu, Z., Huang, Y., Ma, D., Yang, J. and Mays, J.W., **2003**. Characterization of poly(ε-caprolactone) via size exclusion chromatography with online right-angle laser-light scattering and viscometric detectors. *International Journal of Polymer Analysis and Characterization, 8*(6), pp.383–394.
52. Crescenzi, V., Manzini, G., Calzolari, G. and Borri, C., **1972**. Thermodynamics of fusion of poly-beta-propiolactone and poly-ε-caprolactone. Comparative analysis of the melting of aliphatic polylactone and polyester chains. *European Polymer Journal, 8*(3), pp.449–463.
53. Murthy, N., Wilson, S. and Sy, J.C., **2012**. Biodegradation of polymers. *Polymer Science: A Comprehensive Reference*, Amsterdam, The Netherlands, Elsevier, Vol. 9, pp.547–560.
54. Gleadall, A., Pan, J., Kruft, M.A. and Kellomäki, M., **2014**. Degradation mechanisms of bioresorbable polyesters. Part 2. Effects of initial molecular weight and residual monomer. *Acta Biomaterialia, 10*(5), pp.2233–2240.
55. Gleadall, A., Pan, J., Kruft, M.A. and Kellomäki, M., **2014**. Degradation mechanisms of bioresorbable polyesters. Part 1. Effects of random scission, end scission and autocatalysis. *Acta Biomaterialia, 10*(5), pp.2223–2232.
56. Dimiev, A.M., Alemany, L.B. and Tour, J.M., **2013**. Graphene oxide. Origin of acidity, its instability in water, and a new dynamic structural model. *ACS Nano, 7*(1), pp.576–588.
57. Buchsteiner, A., Lerf, A. and Pieper, J., **2006**. Water dynamics in graphite oxide investigated with neutron scattering. *Journal of Physical Chemistry B, 110*(45), pp.22328–22338.
58. Wang, G.S., Zhi-Yong, W., Lin, S., Chen, G., Zhang, W., Dong, X. and Qi, M., **2013**. Morphology, crystallization and mechanical properties of poly(ϵ-caprolactone)/graphene oxide nanocomposites. *Chinese Journal of Polymer Science (English Edition), 31*(8), pp.1148–1160.
59. Hua, L., Kai, W.H. and Inoue, Y., **2007**. Crystallization behavior of poly(ϵ-caprolactone)/graphite oxide composites. *Journal of Applied Polymer Science, 106*, pp.4225–4232.

Received: 2 December 2019. Accepted: 22 January 2020.

Article